Scaling experiments on the dynamics and acoustics of travelling bubble cavitation

Y KUHN DE CHIZELLE, MSc and C E BRENNEN, BA, MA, DPhil
California Institute of Technology, Pasadena, California, United States of America
S L CECCIO, PhD, MASME
University of Michigan, Ann Arbour, Michigan, United States of America
S GOWING, MSc
David Taylor Research Centre, Bethesda, Maryland, United States of America

ABSTRACT Ceccio and Brennen (1991 and 1989) recently examined the interaction between individual cavitation bubbles and the structure of the boundary layer and flow field in which the bubble is growing and collapsing. They were able to show that individual bubbles are often fissioned by the fluid shear and that this process can significantly effect the acoustic signal produced by the collapse. More recently Kumar and Brennen (1991-1992) have closely examined further statistical properties of the acoustical signals from individual cavitation bubbles on two different headforms in order to learn more about the bubble/flow interactions. All of these experiments were, however, conducted in the same facility with the same size of headform (5.08cm in diameter) and over a fairly narrow range of flow velocities (around 9m/s). Clearly this raises the issue of how the phenomena identified change with speed, scale and facility. The present paper describes experiments conducted in order to try to answer some of these important questions regarding the scaling of the cavitation phenomena. The experiments were conducted in the Large Cavitation Channel of the David Taylor Research Center in Memphis Tennessee, on similar Schiebe headforms which are 5.08, 25.4 and 50.8cm in diameter for speeds ranging up to 15m/s and for a range of cavitation numbers.

NOMENCLATURE

C_p	pressure coefficient, $(P_o-P)/(0.5\rho U_o^2)$
D	headform diameter
I*	dimensionless acoustic impulse
P	static local pressure
P_o	static free-stream pressure
P_v	water vapor pressure
R	bubble radius at the base
Re	Reynolds number, U_oD/ν
t	time
U_o	free-stream velocity
γ_i	dimensionless electrode coverage parameter
γ	global coverage parameter
ν	kinematic viscosity
ρ	density
σ	cavitation number, $(P_o-P_v)/(0.5\rho U_o^2)$
σ_i	inception cavitation number
τ_w	acoustic impulse duration

1. INTRODUCTION

The purpose of the experiments described herein was to investigate the effects of scale in the cavitation occurring on a simple axisymmetric headform. The focus is on traveling bubble cavitation, and the interaction between the flow and the dynamics and acoustics of individual bubbles. Experiments by Ceccio and Brennen (1991) on 5.08cm diameter axisymmetric headforms had revealed a surprising complexity in the flow around single cavitation bubbles. Among the phenomena observed during those previous experiments were the fact that the bubbles have an approximately hemispherical shape and are separated from the solid surface by a thin film of liquid. This general conformation persists during the growth phase though, especially with the larger bubbles, the thin film appears to become unstable and may begin to shear off the underside of the bubble leaving a cloud of smaller bubbles behind. On the other hand, the collapse phase is quite complex and consists of at least three processes occurring simultaneously, namely collapse, shearing due to the velocity gradient near the surface and the rolling up of the bubbles into vortices as a natural consequence of the first two processes. These processes tend to produce small transverse vortices with vapor/gas filled cores. It was noted that the collapse phase was dependent on the shape of the headform and the details differed between the ITTC headform (Lindgren and Johnsson, 1966) which possessed a laminar separation and the Schiebe body (Schiebe, 1972; Meyer, Billet and Holl, 1989) which did not. The current investigation employed Schiebe headforms which have a minimum pressure coefficient on the surface of Cp_{min}=-0.78.

Several other features of the flow around individual cavitation bubbles were noted in those earlier experiments and need to be mentioned here. On the ITTC headform, when some of the larger bubbles passed the point of laminar separation they would induce an attached "streak" of cavitation at both the lateral extremes of the bubble (Ceccio and Brennen, 1991, see also Kuhn de Chizelle et al., 1992). These streaks would stretch out as the bubble proceeded downstream, being anchored at one end to a point on the body surface along the laminar separation line and at the other end to the "wing-tips" of the bubble. The main bubble would collapse, leaving the two streaks it induced to persist longer.

One of the important consequences of these variations in the details of the collapse processes is the effect on the noise produced by a single cavitation event (Ceccio and Brennen, 1991; Kumar and Brennen, 1991-1992). Bubble fission can produce several bubble collapses and therefore several acoustic pulses. Presumably this would also effect the cavitation damage potential of the flow. However it is important to reiterate that these earlier experiments were all conducted with 5.08cm diameter headforms and utilized only a very narrow range of tunnel velocities of 8-9m/s. Consequently there are very real questions as to how the observed phenomena might scale with both headform size and with tunnel velocity. The experiments described here represent one effort to answer some of these questions.

We digress briefly to note that questions on the scaling of cavitation have been asked for many years. One set of scaling issues arise because the ratio of the cavitation nuclei size to the headform size change as the headform diameter changes. The other set of scaling issues derives from the complex interactions between the bubbles and the flow close to the headform with which the bubbles interact. Since the flow is Reynolds number dependent, scaling effects will also be caused by the changes in both body size and tunnel velocity.

In a separate paper (Kuhn de Chizelle et al., 1992) we

have presented data on the size, sphericity, population density and collapse location of the traveling cavitation bubbles. We also included data on the location of surface attachment for those bubbles which trigger attached streaks or patches. The present paper will focus on the noise produced by the collapse of these bubbles, on the scaling of that noise and on the relationship between the noise produced and the dynamics of the bubbles.

2. EXPERIMENTAL SETUP

Large Cavitation Channel

The authors were fortunate to have the opportunity to examine some cavitation scaling effects by conducting experiments in a new facility called the Large Cavitation Channel, which has just been constructed for the David Taylor Research Center (Morgan, 1990). Briefly this facility is a very large water tunnel with a working section which is 3.05m x 3.05m in cross-section. It is capable of tunnel speeds above 15m/s and the pressure control allows operation at sufficiently low pressures in the working section to permit cavitation investigations. Polished lucite windows are located along the side walls of the test section and in the corners at the top and bottom.

Headforms

Three Schiebe headforms of diameter 5.08cm, 25.4cm and 50.8cm were machined out of solid blocks of clear lucite and were mounted in the working section as shown in figure 1. The interiors of the headforms were hollowed out in order to place hydrophones in water within the headform and as close as possible to the cavitation. Lucite was chosen for its good acoustical match with water in addition to its electrically insulating properties. The insides of the headforms were filled with water at atmospheric pressure.

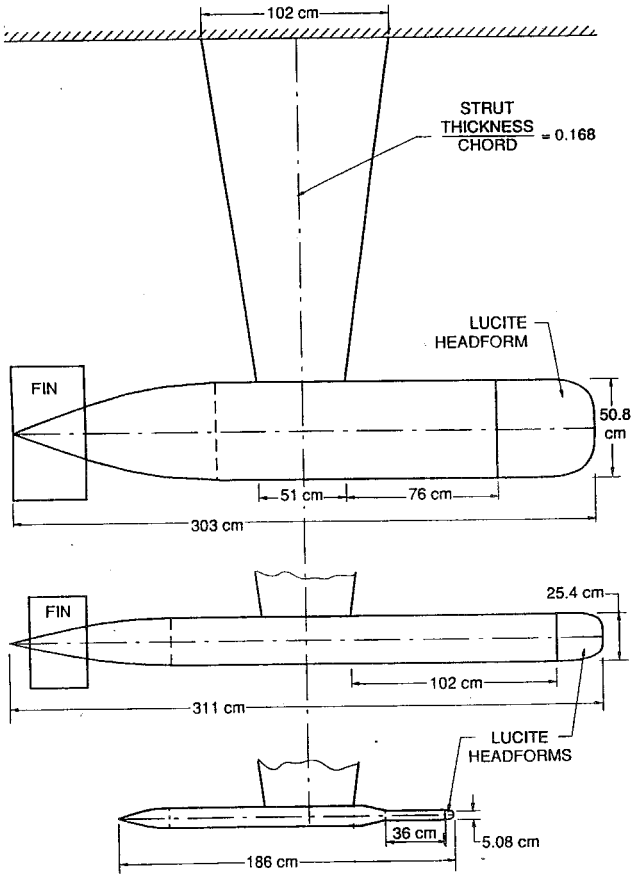

Fig. 1 Schematic diagram the three headforms with afterbodies and supporting strut.

Electrode bubble detection

Silver epoxy electrodes were installed flush in the lucite headform. A pattern of alternating voltages is applied to the electrodes, and the electric current from each is monitored. When a bubble passes over one of the electrodes, the impedance of the flow is altered, causing a drop in current (Ceccio 1989). Thirteen of these electrodes take the form of small patches (about 1mm in diameter) at different axial locations. In addition, three ring electrodes covering the entire circumference of the body were installed at a particular axial location in order to measure the cavitation event rate over the entire headform. A peak detector Schmitt trigger box connected to one of the electrode signal allowed to signal the presence of a traveling bubble.

High speed photography and flash

Two cameras, triggered simultaneously, were set up in order to take flash pictures of individual cavitation bubbles at different angles and different enlargements. Four powerful EGG SS166 flash heads with SS162-165 energy storage racks were used. The film exposure time was of the flash duration and was measured to be about 30μs. Triggering could be done either manually or through a computer controlled lock-out system in series with the electrode peak detector signal. A delay unit was employed in order to take photographs of bubbles at various times after passing an electrode.

In addition, a CCD video camera was focused on the top surface of the headform. The EGG flash heads were used in strobing mode, synchronized with the video camera framing rate in order to make a video recording for each operating condition.

Hydrophones

An ITC-1042 hydrophone with a relatively flat isotropic response out to 80kHz was installed inside each of the headforms. The center of the hydrophone was placed on the axisymmetric axis, one headform radius from the front stagnation point. 64 kbyte long digital signal acquisition were made at a sampling rate of 1MHz with a 16 bit resolution. By filling the interior of the headform with water, the intention was to provide a fairly reflection and reverberation-free acoustic path between the cavitation and the hydrophone. Ceccio (1989) had earlier checked this technique by comparing the signals from a single cavitation event using hydrophones installed inside and outside the headform. In the present tests a similar check was performed by comparing the internal hydrophone signals with those from two STI hydrophones (with a flat frequency response up to 100kHz), installed upstream and downstream from the headform in a water filled recess in the upper wall of the working section. Using each the ITC and STI hydrophones in turn as a transmitter and a receiver over a range of frequency from 1kHz to 100kHz, it was possible to establish the transfer gain spectrum from the inner to the outer hydrophone and vice-versa. Using the manufacturer's response curves for the hydrophones in the receiving and transmitting modes and the theoretical transfer function of the water medium, the mean error on the reciprocity tests over the whole range of measured frequencies proved to be less than 3dB for all three headforms.

Test conditions

The test matrix included three saturation air contents of 80%, 50% and 30% for each of the three Schiebe headforms. The measurements were taken at three velocities of 9m/s, 11.5m/s and 15m/s, allowing a Reynolds number range from 0.54×10^6 to 9.41×10^6. For each velocity about five cavitation numbers were investigated, ranging from bubble inception to fully attached cavitation.

3. CAVITATION INCEPTION DATA

Cavitation inception data was described previously in Kuhn de Chizelle et al. (1992) and will only be summarized here. Inception was defined as the occurrence of some minimum cavitation event rate over the entire body. The

event rate could be monitored by the means of the electrodes located in the region of bubble growth. We arbitrarily defined inception as corresponding to a minimum of one event every 5 seconds detected by the upstream patch electrode.

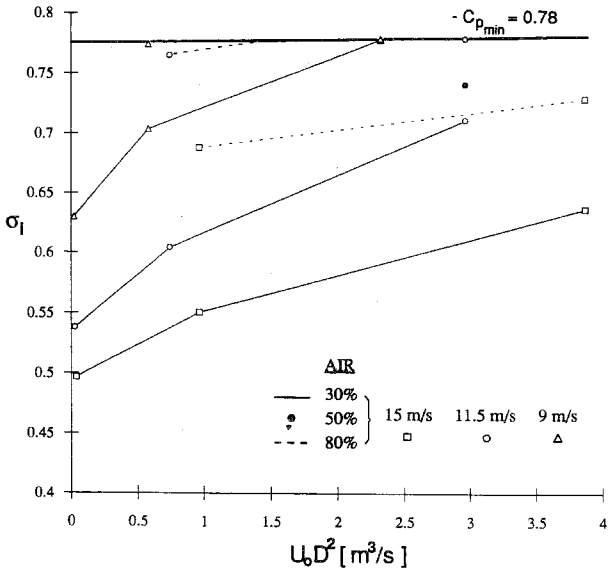

Fig. 2 Cavitation inception numbers σ_i, for the various headform sizes, velocities and air contents.

Data on the cavitation inception numbers, σ_i, are presented in figure 2 for all the velocities, headform sizes and air contents as a function of an equivalent flow rate defined as U_0D^2. The inception cavitation number increases as expected with increasing air contents and headform sizes. For the 80% air content saturation this increase appears limited by the $\sigma=-Cp_{min}=0.78$ value. Inception does not occur above this cavitation number since the pressure in the entire flow field above the headform would be above vapor pressure. In addition however, σ_i decreases markedly with increasing velocity. This unexpected decrease of the cavitation event rate can be partly attributed to the increase in free stream nuclei population due to the lower tunnel pressures required to maintain similar cavitation numbers at higher velocities.

For later reference it is important to observe that when the pressure is sufficiently low for the smallest headform to reach inception, the larger headforms already exhibit quite extensive cavitation patterns. The interesting range of cavitation numbers therefore varies considerably from one headform to another.

4. CAVITATION APPEARANCE

Bubble shape

For cavitation numbers close to the minimum pressure coefficient $-Cp_{min}=0.78$, the bubble life-time is extremely short. Under these conditions all the bubbles assume a very thin disk-like geometry and there is little or no growth normal to the headform surface. At these cavitation numbers potential flow calculations show that the critical isobar $Cp=-\sigma$ appears very elongated and close to the body surface (Kuhn de Chizelle et al., 1992). The region below vapor pressure is quite similar to the shape the bubbles assume. It appears that the bubbles are prevented from growing in the direction perpendicular to the body surface by the high normal pressure gradients.

As the cavitation number is decreased below inception, the bubbles grow in volume (in diameter and in height). Rapidly their growth appears to interfere with the headform surface, and eventually all the bubbles adopt the hemispherical cap shape seen in figure 3a. As the bubbles approach their collapse phase their thickness, δ, normal to the headform surface decreases faster than their base radius, R, and the leading edge collapses most rapidly along a fairly straight front.

One entirely new observation from the current experiments was of the presence of wave-like circular dimples on the top of the bubble (figures 3a, 3b). These seem to become more pronounced as the volume of the bubble increases and this effect which may be related to the Weber number may explain why the dimples were not seen in the earlier experiments on the 5.08cm headform. The dimples seem quite stable, and remain on the bubble until the very last stage of collapse.

Observations of bubbles on all three headforms show that the maximum radius of the base of the hemispherical cap, R, scales linearly with the headform diameter, D (Kuhn de Chizelle et al., 1992). At the same cavitation number, the ratio, r=R/D, appears to be the same for all three headforms. No variation of r with the velocity U_0 have been observed Furthermore the relative collapse location is also approximately the same for all headforms.

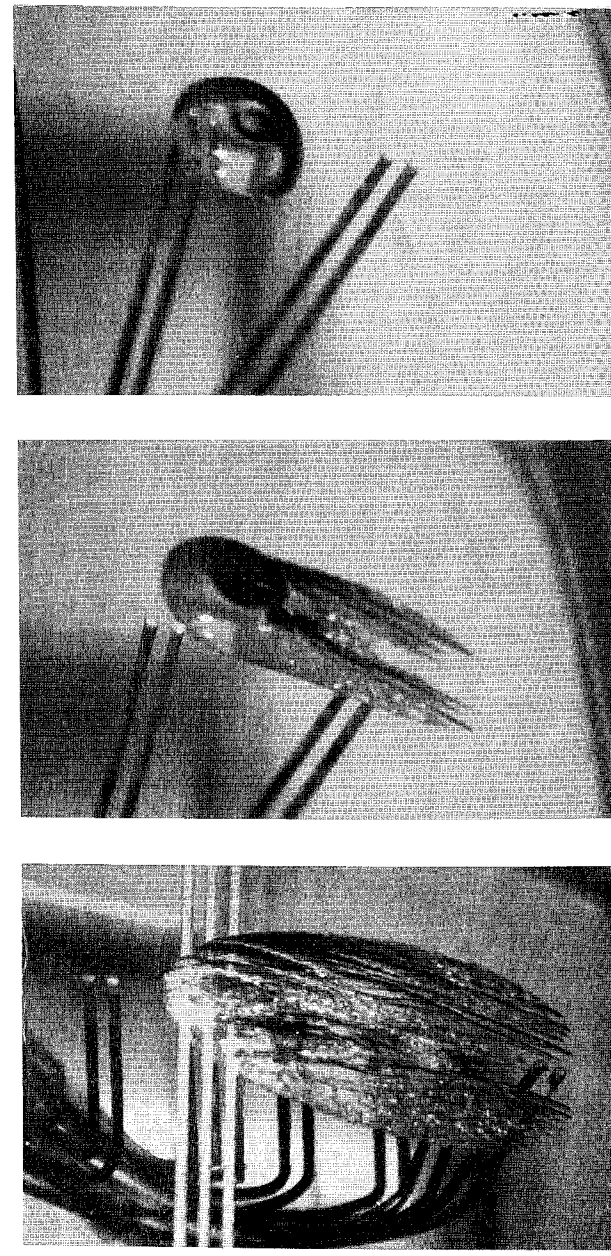

Fig. 3 High speed photography of cavitation events taken on the 50.8cm diameter headform at 30% saturation dissolved air content (distance between the two pairs of patch electrodes: 2.54cm). Figures **a,b**: U_0=15m/s, σ=0.60; Figure **c**: U_0=15m/s, σ=0.55

Bubble streaks and patches

At lower cavitation numbers and on the larger headforms many of the individual bubbles produce streaks of cavitation which are "attached" to the headform at their upstream end and are stretched and grow as the bubble moves downstream (see figure 3b). Ceccio and Brennen (1991) observed such streaks on the ITTC headform where typically a bubble would trigger streaks at the lateral extremes. In the present experiments the frequency of occurrence of attached streaks increased with velocity and headform size (increased Reynolds number) and with cavitation number decrease. Ultimately the larger bubbles will collapse leaving behind patch-like cavities (Fig. 3c).

Whether a bubble will be sheared or not is determined early in its growth phase. If a bubble does not exhibit the trailing edge streaks early in its passage as seen in figure 3b, it will grow and collapse with the smooth cap shape seen in figure 3a. Consequently the leading edge of the patches is always close to the same location on the headform. For small enough cavitation numbers the patch can out-grow the bubble, leaving behind a large patch-like cavity (Fig. 3c).

Bubble-patch interactions

When the cavitation number is sufficiently reduced, the transient patches become fairly stable and remain on the headform, thus creating attached cavities for periods of up to a few seconds. As their number increases the patches will merge to create larger attached structures. The cavitation number at which this phenomenon happens varies considerably from one headform to the other. The transient cavitation patch phenomenon was never observed on the smallest headform, which seemed to exhibit an abrupt switch from traveling bubble cavitation (some of which have long trailing streaks) to persistent attached cavities.

For all test conditions at cavitation numbers below 0.7 we noticed the coexistence of the two different kinds of cavitation patterns: traveling bubbles and transient patches. Quite remarkably, even for the conditions at which we observe many fixed patch-type cavities, some very smooth hemispherical traveling bubbles are still present.

Comparing the shape of the bubbles riding the patch cavities with those which do not, it is clear that the shapes differ because the former are not subjected to the boundary layer shear which the latter experience. Indeed their exterior shape is close to spherical. These bubbles will eventually collapse and merge completely with the attached cavity upstream of its closure region. As will be shown further in this paper, this process greatly affects the noise generation.

Bubble dimensions

Despite the non-spherical nature of the bubbles, for all headforms, the maximum radius at the base of the bubble (next to the headform) is close to the spherical bubble radius predicted by the Rayleigh-Plesset equation. The location of bubble collapse is also quite well predicted by the Rayleigh-Plesset equation. Data on bubble sphericity as measured by the ratio of the height of the bubble normal to the surface to the base radius, has been shown to be a consistent function of the cavitation number for all three headforms (Kuhn de Chizelle et al., 1992).

5. CAVITATION NOISE

Unattached bubble noise

For a range of cavitation numbers between inception and a value at which the cavitation patches persisted, it was possible to identify in the hydrophone output the signal produced by individual bubble collapse. These acoustic pulses were processed in a manner similar to that used by Ceccio and Brennen (1991); some of the processing details were different and need to be mentioned. It was found necessary to digitally high pass filter the signals using a cut-off frequency of 5kHz in order to reduce the effect of vibration and noise caused by cavitation at the top of the supporting strut. This filtering did not, however, substantially effect the results. Secondly the processing amplifier gain response was calibrated and applied to the results.

As in the Ceccio and Brennen (1991) analysis we first examine the acoustic impulse produced by individual bubble collapses. The impulse, I, is defined as the integral under the instantaneous pressure time history from the beginning of the collapse pulse to the moment when the pressure returns to its mean value. Since the impulse will vary inversely with the distance of the hydrophone from the noise source, we multiply I by the appropriate headform radius D/2 and form a dimensionless impulse, I*, by dividing by the headform radius, free stream velocity and the fluid density as indicated by the Rayleigh-Plesset analysis, so that the dimensionless impulse, $I^* = 4\pi I/\rho U_o$. Ceccio and Brennen (1991) showed that on 5.08cm diameter headform, the dimensionless impulse was correlated with the maximum bubble size for a wide range of cavitation numbers and that the experimental values were about one quarter to half of the values predicted by the Rayleigh-Plesset analysis. The smaller bubbles which tended to remain unfissioned yielded less scatter than the larger bubbles for which fission and the production of attached streaks were more likely. These "distortions" tended to decrease the acoustic impulse of collapse. Preliminary inspection of the impulses from the present experiments revealed even greater variability in the acoustic signals from collapse than were observed in the earlier tests with the 5.08cm headform. Indeed it was clear that the bubbles which did not generate attached streaks usually produced the "classical" single pulses with larger values of the impulse.

We examine first this class of bubbles and turn our attention later to the effect of the attached streaks and patches which, typically, lead to smaller acoustic impulses. The hydrophone output for each of the experimental conditions was examined in order to identify at least 40 of the larger pulses associated with a bubble collapse. The average values of the non-dimensional impulses obtained in this way are plotted against cavitation number in figure 4. The standard deviation within each set of measurements is also shown underneath along with the average duration of the pulses.

The non-dimensional impulse is of the same order of magnitude for all three headforms. It initially increases as the cavitation number is decreased below inception. However most of the data also indicates that the maximum impulse ceases to increase and, in fact, decreases when σ is decreased below a certain value (about 0.43, 0.50 and 0.62 for the 5.08cm 25.4cm and 50.8cm diameter headform). The decrease at low cavitation numbers can be explained by the increasing presence of attached cavitation patches, damping the bubble collapse mechanism. The location of the peaks appears to be somewhat influenced by the velocity, and are shifted towards higher cavitation numbers for lower velocities. This trend is consistent with previous observations (Kuhn de Chizelle et al., 1992) of the average void fraction over the headform at constant cavitation numbers, which exhibited an increase with a decrease in velocity. The conditions at which the impulses, I*, are maximum seem to occur for void fractions covering about 20% of the nose of the headform. Higher void fractions will considerably reduce the noise impulses.

The standard deviation for the impulse is substantial, so that the cavitation noise may vary considerably from one event to the other, even for identical cavitation conditions. The duration of the impulse, τ_W, is also presented in figure 4 and reveals a cavitation number dependence similar to the one observed for the impulse. It appears to be of the same order of magnitude for all velocities and diameters. Examining this data it should be recalled that the typical response time of the hydrophone is about 3μs and is not negligible compared with the measured duration.

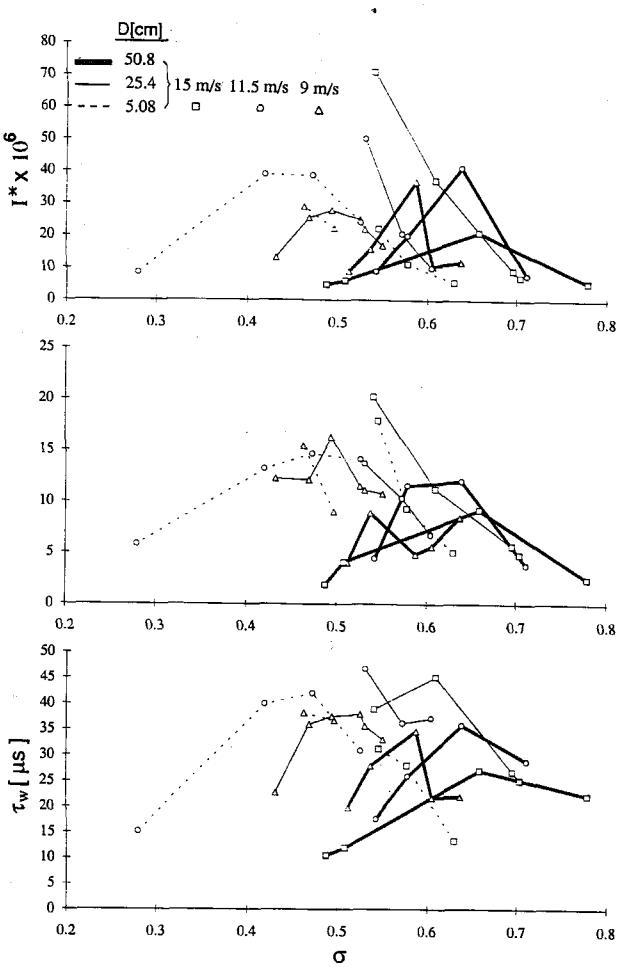

Fig. 4 Average dimensionless maximum acoustic impulse I*, impulse standard deviation and impulse durationτ_w [μs] for all three headforms as a function of the cavitation number.

In summary, we find that unattached traveling bubble noise scales in the way expected on the basis of the Rayleigh-Plesset analysis. The acoustic impulse produced by a single bubble collapse while exhibiting considerable variability nevertheless scales with headform size and tunnel velocity in the way which is expected.

Individual bubble signals

In order to analyze the noise generated by individual bubbles and evaluate the effect of bubble attachment and patch on the production of cavitation noise it is necessary to correlate the bubble geometry with the hydrophone output. This has been accomplished by using the electrode output as well as the photographs as a diagnostic indicating the degree of bubble attachment and correlating them with the simultaneous recording of the hydrophone signal. When a bubble is located over the electrode "i", it produces a perturbation in the signal, $v_i(t)$, from that electrode so that the typical time for which a bubble covers the electrode is given by $\tau_i = \int_{t=0}^{t=\text{end of electrode signal}} v_i(t)dt \Big/ v_{i_{max}}$ and can be written in dimensionless form by defining an electrode coverage parameter $\gamma_i=\tau_i U_0/D$. Clearly a bubble with attached streaks or patches will yield substantially larger γ_i values than single unattached bubbles. Therefore γ_i provides a valuable measure indicating the type of event which is occurring. For single traveling bubbles, the coverage parameters over the first and the second upstream patch electrode (located 5.08cm and 7.62cm downstream of the headform's stagnation point) are strongly correlated. Thus only bubbles appearing to exert the trailing streak pattern as early as the first electrode will have long coverage parameters over electrode 2. The global coverage parameter γ defined as $\gamma = \sqrt{\gamma_1\gamma_2}$ groups both electrode coverage parameters. We then correlate the acoustic output of each event with the γ value for that event in order to explore the effect of bubble attachment on the noise. Figure 5 presents γ as a function of the non-dimensional acoustic impulse I* for the 50.8cm headform at a 30% saturation air content. Most of the data is confined to cavitation numbers close to inception (low event rates) in order to ensure no overlap between events.

This figure leads to several conclusions. First we focus on the data on the left hand side for values of γ less than 0.01. These correspond to unattached bubbles with the smallest bubbles having the smallest values of γ. We can observe that the smallest values of γ correspond to high cavitation numbers (σ>0.7) whereas γ values around 0.01 correspond σ values less than 0.66. For this range of coverage parameter values the maximum impulse increases with increasing bubble size as previously suggested by Fitzpatrick and Strasberg (1956), Hamilton et al. (1982) and Ceccio and Brennen (1991). The impulse can be much smaller than this maximum but an upper bound of the envelope is apparent.

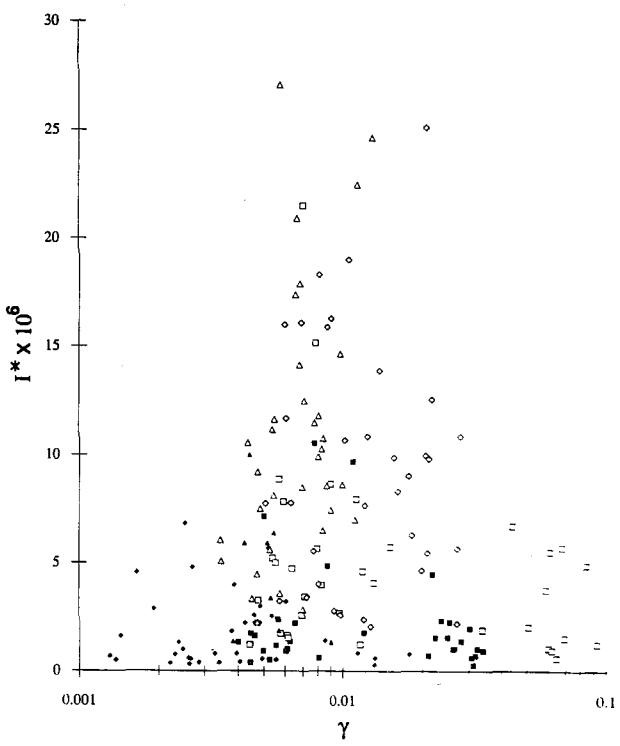

Fig. 5 Dimensionless acoustic impulse, I*, for the 50.8cm headform as a function of the electrode signal coverage parameter γ. Data for: ▪ σ=0.64,U_0=15m/s; □ σ=0.60,U_0=15m/s; ⋄ σ=0.71,U_0=11.5m/s; ◇ σ=0.64,U_0=11.5m/s; ▲ σ=0.78,U_0=9m/s; △ σ=0.66,U_0=9m/s

Finally the data shows a clear decline in the impulse when the values of γ exceed about 0.02. These bubbles are those which have generated attached streaks and patches and

it is apparent that this results in a clear decrease in the impulse associated with the collapse of these events. The largest coverage parameters, γ, correspond to the lowest cavitation numbers and thus to the largest patch cavities. The reduction in cavitation noise can probably be attributed to the fact that the collapse is much less coherent, producing high pressure nodes which are much smaller in magnitude.

6. CONCLUSIONS

In this paper we have presented some of the results from a series of experiments carried out in the Large Cavitation Channel (LCC) to investigate the scaling of the dynamics and acoustics of individual cavitation bubbles in flows around headforms. Many of the phenomena observed by Ceccio and Brennen (1991) in experiments on 5.08cm headforms were seen again in the present experiments. Such micro-fluid mechanical phenomena included the hemispherical shape of individual cavitation bubbles, the thin film separating them from the surface, the destabilization of that film, the occasional production of attached streaks in the wake of the bubbles and the complex processes during the bubble collapse including bubble fission and roll-up into vortices.

The present experiments first revealed substantially lower cavitation inception numbers for the larger headforms. One result of this was that for the same air content, velocity and cavitation number, we observed bubble inception on the smallest headform and fully developed attached cavitation on the largest. Some of the differences in the appearance of individual bubbles on the three headforms could be attributed to this large difference in inception numbers since it implied quite different locations for the critical $C_p=-\sigma$ isobars. The most noticeable effect of scale on the appearance of cavitation was the increase in bubble-generated attached streaks and patches for the larger headforms. On the 5.08cm headform a traveling bubble would occasionally generate two attached streaks or tails at the lateral extremes of the bubble. These would disappear almost immediately after the bubble collapsed. On the larger headforms at higher speeds (larger Reynolds numbers) and low cavitation numbers the streaks began to occur more frequently and extend behind the entire width of the bubble. The streaks would tend to produce a transient patch of attached cavitation which would disappear as the bubble collapses. For low enough cavitation numbers though those patches would persist almost indefinitely and create larger attached cavitation structures. Another new observation during the present experiments was the appearance of a remarkably repeatable "dimple" on the exterior surface of the traveling bubbles on the two larger headforms. These seem to appear when the actual bubble becomes sufficiently large which suggests that they are influenced by surface tension.

In section 6 we discussed how the different cavitation conditions affected the emitted noise. We saw that the pressure impulse could be adequately scaled with the headform diameter and the free flow velocity, in agreement with Rayleigh-Plesset analysis. As expected, lower cavitation numbers lead to higher impulses as long as the interference with larger patch type cavities remained limited. The shearing mechanism of individual bubbles, producing trailing streaks and patch cavities greatly decreased the emitted collapse noise. It appears that these phenomena tend to diffuse the collapse and do not allow the production of high pressure nodes.

ACKNOWLEDGMENTS

Large scale experiments like these require help of many people and the authors are very grateful to all of those who helped in this enterprise. We are very grateful to the ONR for their support under contracts N00014-91-J-1426 (SLC) and N00014-91-J-1295 (CEB, YKdC). We are also extremely grateful to the David Taylor Research Center (DTRC) and to their staff including W.B. Morgan for making the use of the LCC possible for us. From DTRC both Young Shen and James Blanton were important and valued members of the team who conducted the experiments. Po-Wen Yu (U. of Michigan) and Douglas Hart (Caltech) provided important help with the experiments. The staff at the LCC in Memphis, Tenn. were remarkably tolerant and invariably helpful and we wish to thank all of them most sincerely; we are particularly grateful to Bob Etter whose constant support was invaluable.

REFERENCES

Arakeri, V.H. and Shanmuganathan, V. 1985. *On the evidence for the effect of bubble interference on cavitation noise.* J. Fluid Mech., Vol. 159, pp. 131-150.

Brennen, C.E. and Ceccio, S.L. 1989. *Recent Observations on cavitation and cavitation noise.* Proc. ASME Third Int. Symp. on Cavitation Noise and Erosion in Fluid Systems, San Francisco, FED-Vol. 88, pp. 67-78.

Briancon-Marjollet, L. and Franc, J.M. 1990. *Transient bubbles interacting with an attached cavity and the boundary layer.* J. Fluid Mech., Vol. 218, pp. 355-376.

Blake, W.K., Wolpert, M.J. and Geib, F.E. 1977. *Cavitation noise and inception as influenced by boundary layer development on a hydrofoil.* J. Fluid Mech., Vol. 80, pp. 617-640.

Ceccio, S.L. 1989. *Observations of the dynamics and acoustics of traveling bubble cavitation.* Ph.D. Thesis, California Institute of Technology.

Ceccio, S.L. and Brennen, C.E. 1991. *The dynamics and acoustics of traveling bubble cavitation.* J. Fluid Mech., Vol. 233, pp. 633-660.

D'Agostino, L., Brennen, C.E. and Acosta, A.J. 1988. *Linearized dynamics of two-dimensional bubbly and cavitating flows over slender surfaces.* J. Fluid Mech., Vol. 192, pp. 485-509.

Fitzpatrick, H.M. and Strasberg, M. 1956. *Hydrodynamic sources of sound.* First Symp. on Naval Hydrodynamics, Washington D.C., pp. 241-280.

Kumar, S. and Brennen, C.E. 1991. *Statistics of noise generated by traveling bubble cavitation.* ASME Cavitation and Multiphase Flow Forum, Portland OR, June 1991, FED Vol. 109, pp. 55-62.

Kuhn de Chizelle, Y., Ceccio, S.L., Brennen, C.E. and Shen, Y. 1992. *Cavitation scaling experiments with headforms: Bubble dynamics.* Proc. Second International Symposium on Propeller and Cavitation ISPC, Hangzhou, China.

Kumar, S. and Brennen, C.E. 1992. *An acoustical study of traveling bubble cavitation.* Submitted to J. of Fluid Mech.

Lindgren, H. and Johnsson, C.A. 1966. *Cavitation inception on headforms. ITTC comparative experiments.* 11th Int. Towing Tank Conf., pp. 219-232.

Meyer, R.S., Billet, M.L. and Holl, J.W. 1989. *Free-stream nuclei and cavitation.* Proc. ASME Third Int. Symp. on Cavitation Noise and Erosion in Fluid Systems, San Francisco, FED-Vol. 88, pp. 52-62.

Morgan, W.B. 1990. *David Taylor Research Center's Large Cavitation Channel.* Proc. Int. Towing Tank Conference, Madrid, Spain, pp. 1-9.

Schiebe, F.R. 1972. *Measurements of the cavitation susceptibility of water using standard bodies.* St. Anthony Falls Hydraulic Lab., Univ. of Minnesota, Rep. No. 118.

Vogel, A., Lauterborn, W. and Timm, R. 1989. Optical and *acoustic investigations of dynamics of the Laser*-produced cavitation bubbles near a solid boundary layer. J. Fluid Mech., Vol. 206, pp. 299-338.